

# Tidal Influence Upon Flow in Rivers

J. E. BALL<sup>1</sup> and F. M. HENDERSON<sup>2</sup>

<sup>1</sup>Gutteridge Haskins & Davey Pty. Ltd.

<sup>2</sup>University of Newcastle, Australia.

## ABSTRACT

Increasing development along coastal regions has resulted in engineers and water resource managers having to become conversant with the interaction between flow, flood or otherwise, in rivers and the tidal cycle in the ocean. The tidal cycle and its interaction with river flows is an example of unsteady flow. Consequently, determination of the interaction between the tidal cycle and the river flows requires solution of the unsteady flow equations.

This paper presents results from a solution of the non-dimensional unsteady flow equations for alternative tidal and river conditions. Also presented is a summary of the algorithm used for the numerical solution of the non-dimensional unsteady flow equations.

## 1. INTRODUCTION

There are two broad classifications into which flow in open channels can be arbitrarily divided. These two classifications are steady flow and unsteady flow. Water flow in most natural channels is almost always unsteady. At the mouth of a river, the unsteadiness in flow can be introduced either by the action of the tidal cycle or by time variant flow rates in the channel. To determine the interaction between the tidal cycle and the flow in a river it is necessary to solve the dynamic wave equations, commonly referred to as the Saint Venant equations. Numerical algorithms for the dynamic wave equations can be broadly classified as:-

1. characteristic methods using either a fixed spatial grid or a characteristic grid,
2. explicit methods, and
3. implicit methods.

These solution algorithms can be applied to the dynamic wave equations in a dimensional or a non-dimensional form.

The purpose of this paper is to present a summary of an implicit algorithm used to solve a set of non-dimensional dynamic wave equations and, hence, to determine the interaction between the river flow and the tidal cycle. Also presented are the results of a sensitivity analysis showing the influence upon the solution of a number of non-dimensional parameters.

## 2. UNSTEADY FLOW EQUATIONS

One dimensional unsteady flow can be described by two non-linear hyperbolic partial differential equations. Henderson (1966) showed that, for a wide rectangular river, the dynamic wave equations can be expressed as

$$u \frac{\partial y}{\partial x} + y \frac{\partial u}{\partial x} + \frac{\partial y}{\partial t} = 0 \quad (1)$$

$$S_f = S_o - \frac{\partial y}{\partial x} - \frac{u}{g} \frac{\partial u}{\partial x} - \frac{1}{g} \frac{\partial u}{\partial t} \quad (2)$$

where  $y$  is the flow depth,  $u$  is the average velocity,  $x$  is the longitudinal distance along the river (positive downstream),  $t$  is time,  $S_f$  is the friction slope,  $S_o$  is the bed slope and  $g$  is acceleration due to gravity. Using the non-dimensional quantities

$$Y = \frac{y}{y_o} \quad (3)$$

$$U = \frac{u}{u_o} \quad (4)$$

$$X = \frac{x S_o}{y_o} \quad (5)$$

$$T = \frac{t u_o S_o}{y_o} \quad (6)$$

in equations 1 and 2, and rearranging results in the following non-dimensional set of equations,

$$U \frac{\partial Y}{\partial X} + Y \frac{\partial U}{\partial X} + \frac{\partial Y}{\partial T} = 0 \quad (7)$$

$$\frac{S_f}{S_o} = 1 - \frac{\partial Y}{\partial X} - F_o^2 \left[ \frac{U \partial U}{\partial X} + \frac{\partial U}{\partial T} \right] \quad (8)$$

where  $y_o$  is the normal depth of flow,  $u_o$  is the normal flow velocity,  $Y$  is the non-dimensional flow depth,  $U$  is the non-dimensional average velocity,  $X$  is the non-dimensional longitudinal distance,  $T$  is the non-dimensional time, and  $F_o$  is the normal flow Froude number given by

$$F_o^2 = \frac{U_o^2}{g y_o} \quad (9)$$

If the Chezy equation (Henderson 1966) is used to determine the friction slope, i.e.

$$U = C [RS]^{1/2} \quad (10)$$

and it is assumed that, for a wide rectangular channel, the hydraulic radius ( $R$ ) is equal to the flow depth ( $y$ ) then it can be shown that

$$\frac{S_f}{S_o} = \frac{U^2}{Y} \quad (11)$$

Substitution of equation 11 into equation 8 results in

$$1 - \frac{\partial Y}{\partial X} - F_o^2 \left[ \frac{U}{Y} \frac{\partial U}{\partial X} + \frac{\partial U}{\partial T} \right] - \frac{U^2}{Y} = 0 \quad (12)$$

which with equation 7, constitutes a set of partial differential equations in the two non-dimensional dependent variables ( $U$  and  $Y$ ).

### 3. SOLUTION OF UNSTEADY FLOW EQUATIONS

Description of an iterative matrix implicit algorithm with a four-point finite difference scheme for the solution of the dynamic wave equations can be found in many publications, e.g. Fread (1974), Ameen and Chu (1975) and Cunge et al (1980). The essence of the four-point scheme is to express the dynamic wave equations in finite difference form based upon the values at the four-nodes which form the corners of a box, see Figure 1.

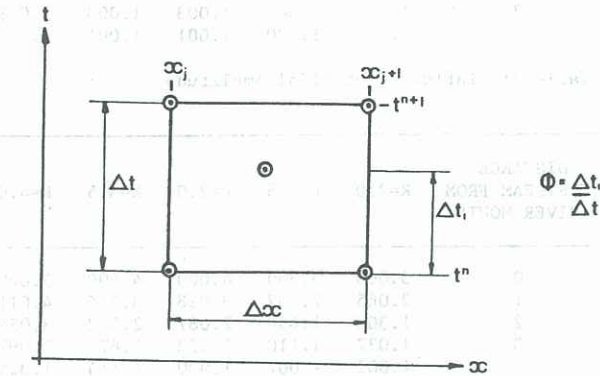


Figure 1: Four Point Implicit Scheme Grid.

Using the finite difference approximation

$$\frac{\partial \alpha}{\partial t} = \frac{1}{\Delta t} \left[ (\alpha_j^{n+1} + \alpha_{j+1}^{n+1}) - (\alpha_j^n + \alpha_{j+1}^n) \right] \quad (13)$$

$$\frac{\partial \alpha}{\partial x} = \frac{1}{\Delta x} \left[ (\phi_{j+1}^{n+1} - \alpha_j^{n+1}) + (1-\phi)(\alpha_{j+1}^n - \alpha_j^n) \right] \quad (14)$$

$$\alpha = \frac{1}{2} \left[ (\phi_{j+1}^{n+1} + \alpha_{j+1}^{n+1}) + (1-\phi)(\alpha_j^n + \alpha_{j+1}^n) \right] \quad (15)$$

equations 7 and 12 can be written as

$$C_j (U_j^{n+1}, Y_j^{n+1}, U_{j+1}^{n+1}, Y_{j+1}^{n+1}) = 0 \quad (16)$$

and

$$M_j (U_j^{n+1}, Y_j^{n+1}, U_{j+1}^{n+1}, Y_{j+1}^{n+1}) = 0 \quad (17)$$

where the subscript and superscript refer to the spatial and temporal locations respectively.

For the case of N nodes along the channel, there are N-1 boxes and 2N unknown variables, i.e. U and Y at each of the N nodal locations. An additional two equations are obtained from consideration of the boundary conditions, i.e.

$$B_o (U_1^{n+1}, Y_1^{n+1}) = 0 \quad (18)$$

$$B_N (U_N^{n+1}, Y_N^{n+1}) = 0 \quad (19)$$

for subcritical flow conditions in the channel.

Solution of the resulting set of 2N nonlinear equations is by utilisation of an iterative matrix technique proposed by Ameen and Fang (1970) which is based upon the use of a generalised Newton-Raphson technique.

#### 4. BOUNDARY CONDITIONS

Only subcritical flow conditions in the river channel were of interest in this study. Consequently the required boundary conditions consisted of one relationship at both the upstream and downstream boundaries of the channel.

#### Upstream Boundary Condition

At the upstream extremity of the river channel, the boundary condition used was a requirement for normal flow conditions to occur. This requirement can be expressed algebraically as

$$S_f - S_o = 0 \quad (20)$$

Rearrangement of equation 20 and substitution of equation 11 results in

$$\frac{U^2}{Y} - 1 = 0 \quad (21)$$

which was the upstream boundary condition used in the study reported in this paper.

#### Downstream Boundary Condition

At the downstream extremity of the channel, the boundary condition used was a relationship between the depth in the channel and the time, i.e.

$$Y = f(T) \quad (22)$$

To approximate the tidal cycle, a sinusoidal relationship was used. This relationship took the form of

$$Y = K + A \sin \left[ \frac{2\pi T}{\sigma} \right] \quad (23)$$

where K is the depth of flow in the channel at mean sea level, A is the amplitude of the tidal cycle, and  $\sigma$  is the tidal period.

#### 5. APPLICATION OF MODEL

The model discussed in the preceding sections was used to determine the interaction between the tidal cycle and river flows for alternative values of the following parameters:-

1.  $F_o$  - Froude number of normal flow in the river,
2. A - amplitude of the tidal cycle,
3.  $K_o$  - flow depth in the river at mean sea level,
4.  $\sigma$  - tidal period.

In each series of tests, one of the above four parameters was varied while the other three retained constant values. Consequently from the four series of tests undertaken, an assessment of the influence of the four non-dimensional parameters can be obtained.

The first test considered the influence of the tidal period upon the predicted peak depth along the channel. Shown in Table 1 are the predicted peak non-dimensional depths along the channel for non-dimensional tidal periods of 10, 20, 30 and 40. Investigation of Table 1 reveals minimal variation in the predicted non-dimensional peak depths.

The next test considered the influence upon the predicted peak non-dimensional depth of the Froude number. For the four alternative numbers considered, i.e.  $F_o^2 = 0.05, 0.01, 0.005$  and  $0.001$ , the peak non-dimensional depths predicted along the channel are shown in Table 2. Similar to the influence of the tidal period, the magnitude of the Froude number does not significantly influence the predicted peak depths along the channel.



DISTANCE UPSTREAM FROM RIVER MOUTH	$\sigma = 10$	$\sigma = 20$	$\sigma = 30$	$\sigma = 40$
0	3.000	3.000	3.000	3.000
1	2.057	2.061	2.063	2.063
2	1.287	1.296	1.300	1.299
3	1.020	1.022	1.024	1.024
4	1.001	1.001	1.002	1.002
5	1.000	1.000	1.001	1.001
6	1.000	1.000	1.000	1.000
7	1.000	1.000	1.000	1.000
8	1.000	1.000	1.000	1.000

Table 1: Influence of Tidal Period

DISTANCE UPSTREAM FROM RIVER MOUTH	$F^2 = 0.05$	$F^2 = 0.01$	$F^2 = 0.005$	$F^2 = 0.001$
0	3.000	3.000	3.000	3.000
1	2.062	2.065	2.065	2.065
2	1.299	1.307	1.308	1.308
3	1.023	1.027	1.027	1.027
4	1.002	1.002	1.002	1.002
5	1.001	1.001	1.001	1.000
6	1.000	1.000	1.000	1.000
7	1.000	1.000	1.000	1.000
8	1.000	1.000	1.000	1.000

Table 2: Influence of Froude Number

The last two test series considered the influence of the non-dimensional amplitude of the tidal cycle and the non-dimensional depth at the mouth of the river channel at mean sea level. Peak non-dimensional depths along the channel predicted during these two test series are shown in Figure 2 and 3 respectively. Investigation of Figure 2 reveals that the predicted non-dimensional depths, for the alternative tidal amplitude considered, have a consistent variation from each other in the lower reaches of the river, i.e. the predicted depths plotted as a function of their location result in a series of parallel lines. As the magnitude of the amplitude increases, this effect extends further upstream. In all cases the variation between the predicted non-dimensional depths was identical to the difference in the non-dimensional tidal amplitude. For the alternative tidal amplitudes considered, i.e.  $A = 0.5$ ,  $1.0$ ,  $1.5$ ,  $2.0$  and  $2.5$ , the predicted depths along the channel are detailed in Table 3.

Consideration of Figure 3, which shows the variation in the predicted non-dimensional peak depth along the channel with a variation in the non-dimensional parameter  $K$ , reveals a similar influence. In the lower reaches of the river, the variation in  $K$  results in similar variations in the predicted non-dimensional depths of all five values of  $K$  considered, i.e.,  $K = 2.0$ ,  $2.5$ ,  $3.0$ ,  $3.5$ ,  $4.0$ . Detailed in Table 4 are the predicted depths along the river channel for the alternative values of the non-dimensional parameter  $K$ .

## 6. CONCLUSION

A numerical model which solves the non-dimensional unsteady flow equations has been developed to consider the interaction between the flow in a river channel and the action of the tidal cycle. This model was used to determine the sensitivity of the model to four non-dimensional parameters, the normal flow Froude number, the period of the tidal cycle, the amplitude of the tidal cycle and the non-dimensional depth at the mouth of the river channel for mean sea level conditions. It was found that for the first two non-dimensional parameters, i.e. the normal flow Froude number and the tidal period, there were minimal variations in the predicted peak depths along the channel.

DISTANCE UPSTREAM FROM RIVER MOUTH	$A=0.5$	$A=1.0$	$A=1.5$	$A=2.0$	$A=2.5$
0	4.000	5.000	5.500	6.000	6.500
1	3.516	4.011	4.508	5.005	5.504
2	2.558	2.097	2.559	3.039	3.528
3	1.671	2.097	1.675	2.101	2.566
4	1.115	1.329	1.675	1.334	1.689
5	1.008	1.031	1.117	1.334	1.689
6	1.001	1.003	1.009	1.037	1.143
7	1.000	1.001	1.003	1.009	1.039
8	1.000	1.000	1.001	1.001	1.009

Table 3: Influence of Tidal Amplitude

DISTANCE UPSTREAM FROM RIVER MOUTH	$K=2.0$	$K=2.5$	$K=3.0$	$K=3.5$	$K=4.0$
0	3.000	3.500	4.000	4.500	5.000
1	2.065	2.537	3.028	3.515	4.011
2	1.308	1.658	2.087	2.552	3.034
3	1.027	1.110	1.323	1.670	2.097
4	1.002	1.007	1.030	1.114	1.329
5	1.001	1.001	1.003	1.008	1.031
6	1.000	1.000	1.003	1.008	1.031
7	1.000	1.000	1.000	1.000	1.001
8	1.000	1.000	1.000	1.000	1.000

Table 4: Influence of Entrance Depth

## REFERENCES

- Amein, M. & Chu, H.L. (1975), 'Implicit Numerical Modelling of Unsteady Flows', *A.S.C.E. Journal of Hydraulics Division*, Vol 101, pp 717-732.
- Cunge, J.A., Holly, F.M. Jr., & Verwey, A. (1980), 'Practical Aspects of Computational River Hydraulics'. Pitman Publishing Ltd.
- Fread, D.L. (1974) 'Numerical Properties of Implicit Four-Point Finite Difference Equations of Unsteady Flow', *NOAA Technical Memo NWS Hydro-18*, U.S. Dept. of Commerce.
- Henderson, F.M. (1966), 'Open Channel Flow' Macmillan Publishing Co.

## NOTATION

- $A$  - Tidal Cycle Amplitude  
 $B_N$  - Downstream Boundary Condition  
 $B_O$  - Upstream Boundary Condition  
 $C$  - Chezy Resistance Coefficient  
 $C_c$  - Continuity Equation  
 $F_o$  - Normal Flow Froude Number  
 $g$  - gravitational acceleration  
 $K$  - flow depth for mean sea level at downstream boundary  
 $M_j$  - Momentum Equation  
 $R_j$  - Hydraulic Radius  
 $S_f$  - Friction Slope  
 $S_b$  - Bed Slope  
 $T_o$  - Non-dimensional Time  
 $t$  - time  
 $U$  - Non-dimensional velocity  
 $u$  - Velocity  
 $u_o$  - Normal flow velocity  
 $X_o$  - Non-dimensional longitudinal distance  
 $x$  - Longitudinal distance  
 $Y$  - Non-dimensional flow depth  
 $y$  - Flow depth  
 $y_o$  - Normal flow depth  
 $\sigma$  - Tidal period

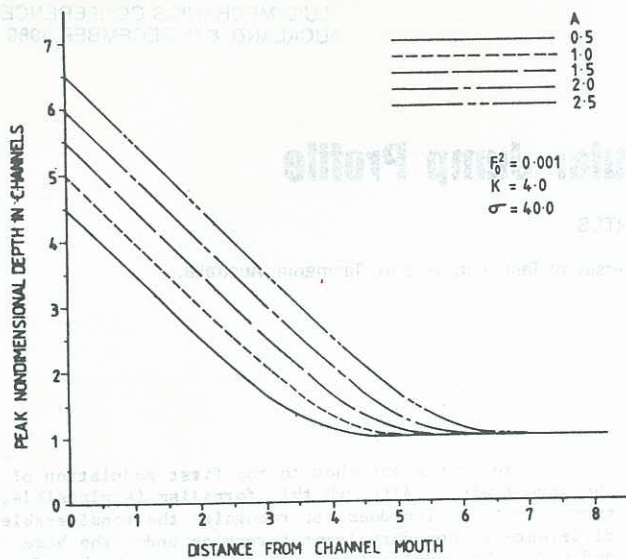


Figure 2: Peak Non-Dimensional Depth Along Channel for Varying Tidal Amplitude

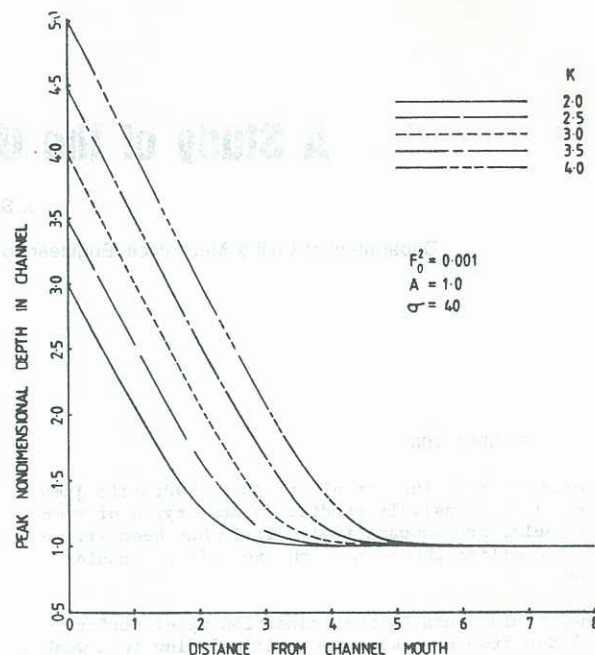


Figure 3: Peak Non-Dimensional Depth Along Channel for Varying Flow Depth at Mean Sea Level

